



Cite this: Analyst, 2015, 140, 2134

Raman microspectroscopy of noncancerous and cancerous human breast tissues. Identification and phase transitions of linoleic and oleic acids by Raman low-temperature studies†

Beata Brozek-Pluska,* Monika Kopec, Jakub Surmacki and Halina Abramczyk

We present the results of Raman studies in the temperature range of 293–77 K on vibrational properties of linoleic and oleic acids and Raman microspectroscopy of human breast tissues at room temperature. Our results confirmed the significant role of unsaturated fatty acids in differentiation of noncancerous and cancerous breast tissues and the role of vibrational spectroscopy in phase transition identification. We have found that vibrational properties are very sensitive indicators to specify phases and phase transitions typical of unsaturated fatty acids at the molecular level. Using Raman spectroscopy we have identified high-temperature, middle-temperature and low-temperature phases of linoleic acid. Results obtained for linoleic acid were compared with parameters characteristic of α and γ phases of oleic acid – the parent compound of polyunsaturated fatty acids.

Received 17th October 2014,
Accepted 11th February 2015
DOI: 10.1039/c4an01877j
www.rsc.org/analyst

Introduction

Polyunsaturated fats can have a positive effect on human health when consumed in moderation and when eaten to replace saturated and *trans* fats in a diet. In the human body fatty acids are important sources of 'fuel' because their metabolism yields large quantities of ATP used by different types of cells in their life cycle.^{1,2} In particular, heart and skeletal muscles prefer fatty acids rather than glucose as an energy source. Oleic acid is a monounsaturated ω -9 fatty acid found in various animal and vegetable fats, and what is relevant to this study, is a parent acid of many polyunsaturated fatty acids (PUFA) like linoleic acid (LA), α -linolenic acid (ALA), eicosapentaenoic acid (EPA), and docosahexaenoic acid (DHA) from the ω -3 family, and γ -linolenic acid (GLA), dihomo- γ -linolenic acid (DGLA) and arachidonic acid (AA) from the ω -6 family.^{2,3} The most important role of PUFA in humans is that they are precursors of eicosanoids, also called tissue hormones.^{2–9} These very unstable, rapidly decomposing substances can act as a triggering factor for cancerous changes.^{10–15} The type and amount of the synthesized eicosanoids are dependent on the availability of the precursor, and the activity of phospholipases

A2 and C, cyclooxygenase and lipoxygenase. AA is a precursor of eicosanoids having the highest biological activity even in very small quantities. Eicosanoids produced via AA metabolism stimulate the development of atherosclerosis, thrombus formation, severe inflammation and allergic reactions, as well as cell proliferation and growth of cancer tissue, especially in the mammary gland, colon and prostate, but polyunsaturated fatty acids can also play a protective role in cancer risk, and the positive role of OA, LA, DHA and EPA in breast cancer risk has been proven in clinical trials.^{16–26}

Even if the dietary factor contribution to the etiology of cancer has not been established unequivocally some research on social groups with varied eating habits show the correlation between the regional differences of breast cancer risk and diet. The fatty acid composition in breast tissue was directly associated with mammary cancer growth in many studies in animals and human cell lines.^{27,28} *cis*-Polyunsaturated fatty acids such as LA and AA are also abundant in brain and retinal tissues for special properties originated from the *cis*-olefin group. Their unsaturation plays a very important role in physical properties of biomembranes, nervous and optical systems in humans.^{29–33}

The distribution and chemical characterization of fatty acids can be monitored in human tissues using Raman microspectroscopy. Raman mapping allows tracking of subcellular structures rich in lipids and fatty acids and represents the ideally suited technique to monitor inhomogeneous distribution of different tissue components. The advantage of

Lodz University of Technology, Institute of Applied Radiation Chemistry, Laboratory of Laser Molecular Spectroscopy, Wroblewskiego 15, 93-590 Lodz, Poland.

E-mail: brozek@mitr.p.lodz.pl; Fax: +48 42 6840043; Tel: +48 42 6313188

† Electronic supplementary information (ESI) available. See DOI: 10.1039/c4an01877j

Raman spectroscopy as compared to other techniques is that no preparation of the tissue samples is needed and many compounds can be tracked simultaneously. Fatty acids are characterized by many intense Raman peaks and the level of unsaturation of these acids can also be easily monitored.^{34–36}

In this paper we would like to focus on structural and conformational changes at the molecular level of selected PUFA because such properties are still unknown and are crucial for their functions in biological systems.

Many lipid compounds with unsaturated acyl chains form several polymorphic phases that are sensitive to the number and the position of the double C=C bond.^{37–44} Vibrational spectroscopy was used in the past for investigations concerning the phase transitions of palmitoleic, erucic and oleic acids. On the basis of spectroscopy and other physical methods (DSC, density, viscosity, self-diffusion), it has been suggested that OA forms a quasi-smectic liquid crystal structure in the temperature range from the melting at 15 °C to about 30 °C, and the structure between 30 °C and 55 °C consists of clusters with a less ordered structure, while the structure above 55 °C appears to be an isotropic liquid. Below the melting temperature oleic acid exists in three solid state phases: α, β, and γ. They have been identified by X-ray diffraction, vibrational spectroscopy, and DSC. It has been found that the α–γ transition occurs at –2.2 °C and represents a disorder–order transition, where in the α phase, the alkyl chain on the methyl side of the C=C bond exhibits conformational disorder, while the segment on the carboxyl-side of the C=C bond remains in the ordered all-trans conformation. The γ phase represents a more ordered structure, in which the unit cell is pseudo-orthorhombic (space group $P2_1/a$) with four molecules (or two hydrogen bonded dimers) per unit cell. The molecules are bent at the C=C bond, and the hydrocarbon chains pack according to the orthorhombic $O\bar{I}I'$ subcell (space group $Pma2$). The β phase exists in two modifications: stable β1 and metastable β2. In the β1 phase the unit cell belongs to a triclinic system of $\bar{P}\bar{1}$ where the asymmetric unit contains two crystallographically independent molecules A and B. The molecular layer exhibits a unique interdigitated structure, where the methyl group of the molecule A and the carboxyl group of the molecule B are located in the same plane. The methyl- and the carboxyl-sided chains together form a $T\parallel$ subcell. The β phase is unique, and has been found only in oleic acid and does not show an order–disorder type solid-state transition.^{3,5,44–46}

Biological functions of linoleic acid have been investigated for elucidating its physiological and pathological roles also using different experimental methods including FTIR spectroscopy. However, the dynamical properties of LA have been under investigation. DSC and XRD experiments confirm that LA forms three phases known as low temperature (LT), middle temperature (MT) and high temperature (HT) phases in the temperature region of –100 °C to –5 °C. On heating the LT phase transforms to the MT phase at –51.3 °C and the MT phase transforms to the HT phase at –33.5 °C respectively. The thermodynamic parameters of both solid-state reversible phase transitions show that the enthalpy of the MT/HT phase

transition is significantly smaller 0.26 kJ mol^{–1} than that of the LT/MT transition equal to 2.6 kJ mol^{–1} suggesting that the most important structural changes take place in the LT/MT transition. Both values are smaller than the enthalpy of the α/γ phase transition of OA equal to 8.76 kJ mol^{–1}.^{47–50}

The main goal of the present study is to investigate the structural changes in the LT/MT and MT/HT phase transitions of LA by low-temperature Raman spectroscopy and to discuss results with data obtained in our group for oleic acid.³⁵ In this paper we have also used Raman microspectroscopy at room temperature 293 K to investigate cancerous and noncancerous human breast tissues to correlate the lipid profile of these tissues with Raman spectra of OA and LA at 293 K.

We do believe that the presented results should not only help in understanding the molecular mechanisms that drive cancerous changes but also prove that vibrational spectroscopy can be used to follow phase transitions of biologically important fatty acids.

Experimental methods

Unsaturated fatty acids

Unsaturated fatty acids, oleic acid (product number O1008) and linoleic acid (product number L1367) were purchased from Sigma-Aldrich and used without purification.

Patients and samples

We examined human breast cancer specimens (infiltrating ductal carcinoma). The breast tissue samples were obtained during a surgical operation. The research did not affect the course of the operation or treatment of the patients. The total number of patients was 232. The total number of samples was 464. For each patient the breast tissue from the safety margin and the tumor mass were measured and analyzed. The typical results of one of the patients have been used to illustrate the essential findings of research. To visualize and identify tissue structures we have used Raman imaging. We avoided the standard steps in the histology protocols, such as formalin fixation, paraffin-embedding, and coating to adhere the cover glass to the microscope slide, on Raman measurements. We observed that using the standard chemical fixative to preserve the tissue from degradation, *i.e.* 10% neutral-buffered formalin (4% formaldehyde in phosphate-buffered saline), did not introduce essential changes in the Raman spectra. This conclusion is based on a comparison between the results obtained using fresh tissue samples (>160 patients) and those obtained using formalin-fixed tissue samples (>60 patients). In contrast, paraffin embedding was not an appropriate protocol for use in Raman measurements. The paraffinization protocol contains steps, such as alcohol dehydration, xylene clearance, and paraffin wax infiltration, and embedding that might introduce artifacts in Raman spectra. We observed that the use of frozen sections (cryosectioned samples), in which the frozen fresh tissue (or formalin-fixed tissue) is sliced into thin sections

(16 μm) using a microtome, is the most appropriate protocol for Raman measurements. The fresh tissue obtained during surgery was snap frozen in liquid nitrogen. The frozen blocks of fresh tissue were stored at -80°C until further processing. The thin slices without staining were placed on CaF_2 windows for Raman measurements. The adjacent sections of tissue were mounted on glass slides, stained with H&E and covered with another layer of glass using a specific adhesive (Histokitt, Glaswarenfabrik Karl Hecht GmbH & Co KG, CAS: 1330-20-7) for histological examination. After obtaining the Raman measurements, trained pathologists examined and stained the slices. As the quality of the slides produced from the frozen sections was lower than that obtained in the standard procedure, standard histological processing using wax-embedded tissue was additionally performed to obtain a more accurate diagnosis for each patient. Professional medical doctors, a board certified as pathologists, from the Medical University of Lodz, Department of Pathology, Chair of Oncology performed and analyzed the histological images. All procedures were conducted under a protocol approved by the Bioethical Committee at the Medical University of Lodz (RNN/45/14/KE/11/03/2014).⁵¹

Instrumentation

All Raman images and spectra reported in this study were acquired using a Ramanor U1000 Raman spectrometer (Jobin Yvon) excited with an Ar ion laser (514 nm) and with an alpha 300 RA (WITec, Ulm, Germany) model equipped with an Olympus microscope coupled *via* the fiber of 50 μm core diameter to an UHTS (Ultra High Throughput Spectrometer) spectrometer and a CCD camera Andor Newton DU970N-UVB-353 operating in standard mode with 1600×200 pixels at -60°C with full vertical binning. The incident laser beam (doubled SHG of the Nd:YAG laser (532 nm)) of alpha 300 RA was focused on the sample through a $40\times$ dry objective (Nikon, objective type CFI Plan Fluor C ELWD DIC-M, numerical aperture (NA) of 0.60 and a 3.6–2.8 mm working distance) to the spot of 600 nm. The average laser excitation power was 10 mW, with an integration time of 0.03 s. Rayleigh scattered light was removed using an edge filter. A piezoelectric table was used to record Raman images. Spectra were collected at one acquisition per pixel and 1200 lines per mm diffraction grating. Each spectrum was processed to remove cosmic rays, and increase the signal-to-noise ratio *via* spectral smoothing (Savitzky–Golay method). Data acquisition and processing were performed using WITec Project 2.10.

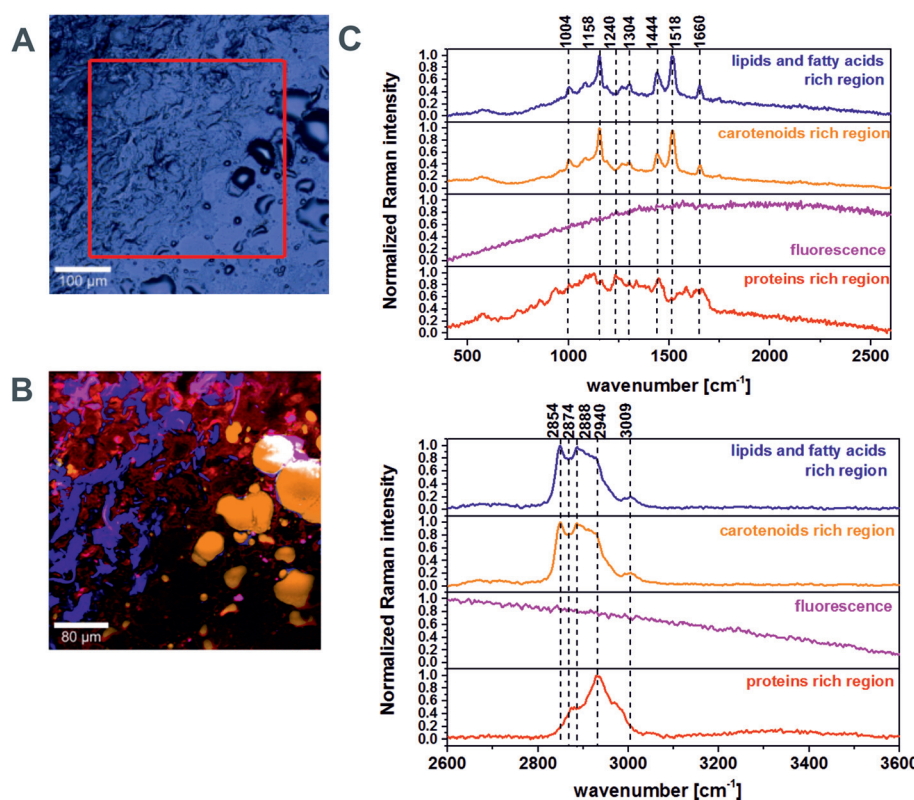


Fig. 1 Microscopy, Raman images and Raman spectra of the noncancerous breast tissue of patient P80. (A) Microscopy image ($500 \times 500 \mu\text{m}$) composed of several single video images of the noncancerous breast tissue, (B) Raman image ($350 \times 350 \mu\text{m}$) of the cryosectioned noncancerous tissue from the region marked in (A) obtained by the basis analysis, (C) Raman spectra of the noncancerous breast tissue. The colours of the Raman spectra correspond to the colours in the Raman image. Mixed areas are displayed as mixed colours. Integration time: 0.03 s.³⁶

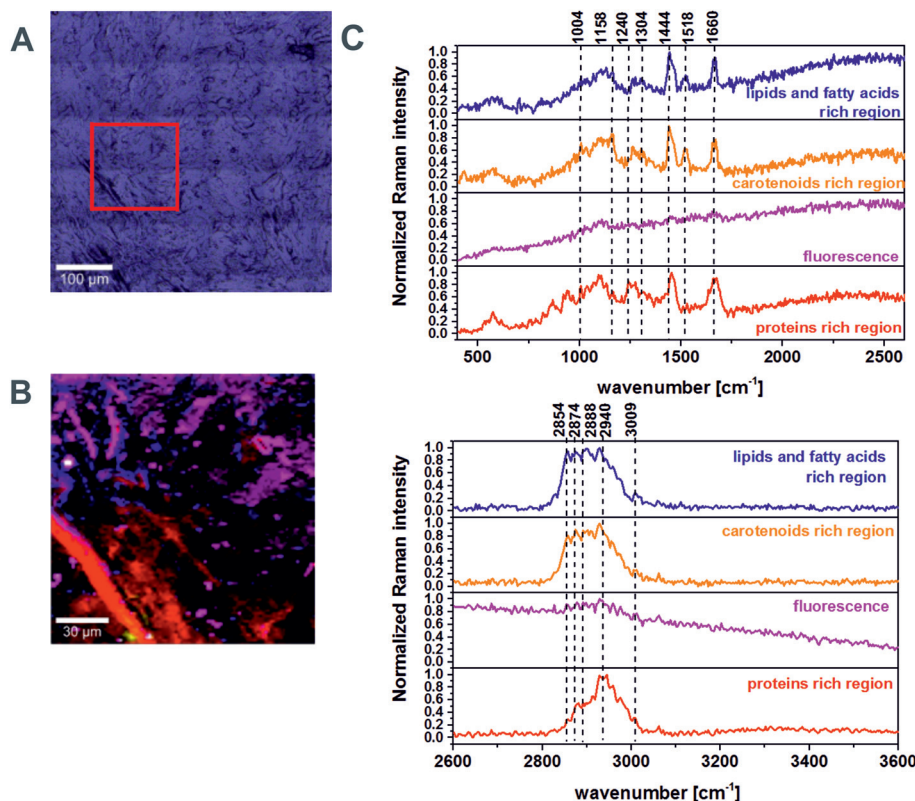


Fig. 2 Microscopy, Raman images and Raman spectra of the cancerous breast tissue (infiltrating ductal cancer, G3) of the patient P80. (A) Microscopy image ($500 \times 500 \mu\text{m}$) composed of several single video images of the cancerous breast tissue, (B) Raman image ($150 \times 150 \mu\text{m}$) of the cancerous cryosectioned tissue from the region marked in (A) obtained by basis analysis, (C) Raman spectra of the cancerous human breast tissue. The colours of the spectra correspond to the colours in the image. Mixed areas are displayed as mixed colours. Integration time: 0.03 s .³⁶

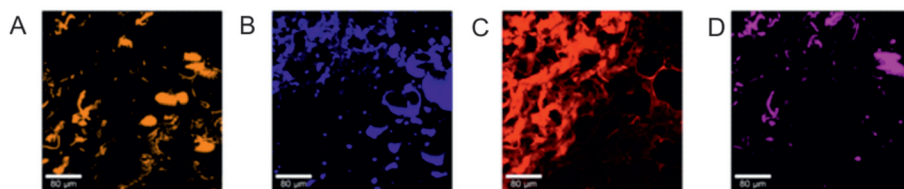


Fig. 3 Images for the filters for spectral regions: (A) $1500\text{--}1550 \text{ cm}^{-1}$, (B) $2850\text{--}2950 \text{ cm}^{-1}$, (C) $2950\text{--}3010 \text{ cm}^{-1}$ and (D) $1800\text{--}2000 \text{ cm}^{-1}$ typical of carotenoid, lipid, protein vibrations and autofluorescence of the noncancerous human breast tissue, P80.

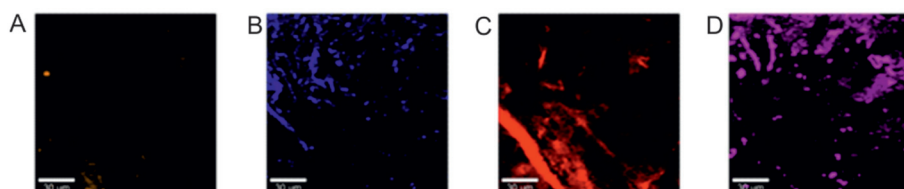


Fig. 4 Images for the filters for spectral regions: (A) $1500\text{--}1550 \text{ cm}^{-1}$, (B) $2850\text{--}2950 \text{ cm}^{-1}$, (C) $2950\text{--}3010 \text{ cm}^{-1}$ and (D) $1800\text{--}2000 \text{ cm}^{-1}$ typical of carotenoid, lipid, protein vibrations and autofluorescence of the cancerous human breast tissue, P80.

Results and discussion

In this section, the results of the Raman studies on the noncancerous and cancerous human breast tissues of the same patient P80 are presented.

The typical Raman spectra of the noncancerous and cancerous (infiltrating ductal cancer, G3) breast tissues are presented in Fig. 1 and 2.

One can see from Fig. 1 and 2 that the lipid profile in the spectral region $2600\text{--}3200 \text{ cm}^{-1}$ for noncancerous tissue is

dominated by the peaks at around 2854, 2874, and 2888 cm^{-1} and the peak at 3009 cm^{-1} ($=\text{C}-\text{H}$) is also easily observed. This observation confirms that the lipid profile for the non-cancerous tissue is dominated by unsaturated fatty acids and their derivatives (esters for example), while the Raman spectra of the cancerous human breast tissue are dominated by proteins for which the peak at around 2940 cm^{-1} is the most characteristic.^{36,52-55}

To monitor the accumulation and spatial distribution of the individual components in the noncancerous and cancerous breast tissues, carotenoids, lipids, fatty acids, and proteins, Raman filters presented in Fig. 3 and 4 were used. The spectral region 1500–1550 cm^{-1} is typical of carotenoids, 2850–2950 cm^{-1} correspond to fatty acids and lipids and 2950–3010 cm^{-1} correspond to protein and lipid vibrations respectively. The autofluorescence of the tissue was estimated using a filter at 1800–2000 cm^{-1} .

The results presented in Fig. 3 and 4 clearly indicate that Raman mapping is a suitable technique to monitor qualitatively and quantitatively (the quantitative analysis is beyond the scope of this paper) the composition of human breast tissues and many compounds can be monitored simultaneously. The comparison of the results for different filters shows that in the noncancerous tissue a high level of carotenoids, which are almost absent in a cancerous human breast tissue sample, can be observed. In regions rich in carotenoids a high concentration of lipids, fatty acids and their derivatives is also noticed. Simultaneously in sample areas rich in lipids, fatty acids and their derivatives a lower concentration of proteins is observed. In addition, the higher fluorescence is typical of the cancerous human breast tissue.

Because we have confirmed that the fatty acids play an important role in carcinogenesis it is reasonable to compare the lipid profile of the cancerous and noncancerous human breast tissues with the Raman spectra of selected fatty acids: LA and OA. A detailed comparison of Raman spectra of the breast tissues, and selected oleic acid and linoleic acids is presented in Fig. 5.

One can see from Fig. 5 that the average Raman spectrum of the noncancerous human breast tissue contains all bands characteristic of selected unsaturated acids. This observation confirms the indisputable role of these acids in the composition of such a type of tissue, originating from the adipose tissue content. In contrast such similarities are not observed for the cancerous tissue. The Raman spectrum of the cancerous tissue is dominated by a peak at around 2940 cm^{-1} which can be described as a combination of the vibrations of saturated lipids and proteins^{35,51} (see Table S1 in the ES[†]).

Having reached this point, when we proved that unsaturated fatty acids play a very important role in differentiation of the normal and the pathologically changed human breast tissues we can ask the question whether we can obtain any information about conformational properties of selected linoleic and oleic acids using Raman spectroscopy.

To gain more information on conformational properties and phase transitions we have investigated Raman spectra of

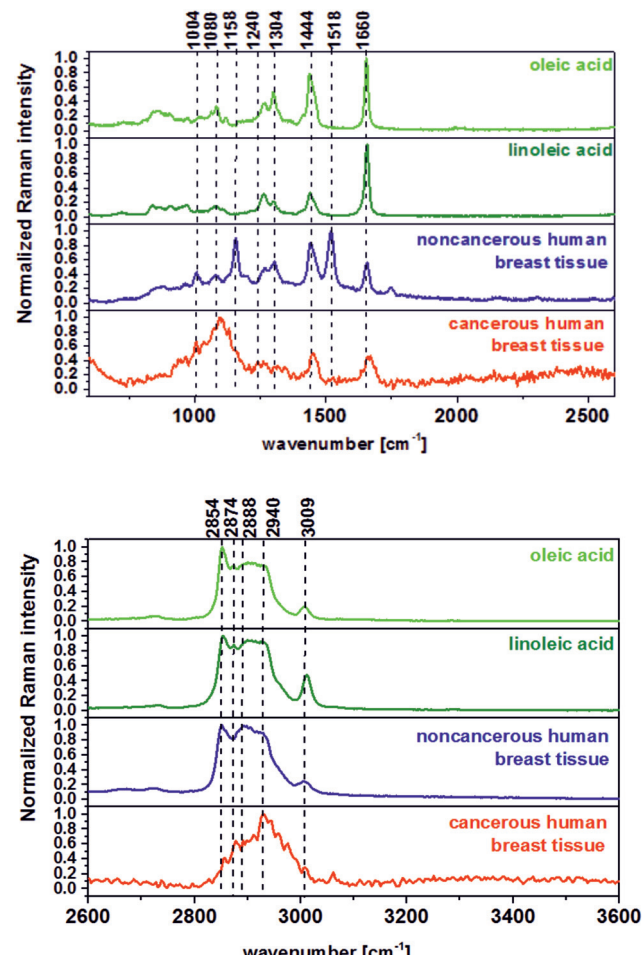


Fig. 5 Comparison of average Raman spectra of the noncancerous and cancerous breast tissues of patient P80, oleic and linoleic acids.

OA and LA as a function of temperature in the range of 293–77 K.

We will demonstrate that the detailed structural evolution of acid chains for LA and OA can be elucidated by analyzing the vibrational spectra of C–H, $=\text{C}-\text{H}$ and C=C modes. Fig. 6 presents the Raman spectra of LA and OA as a function of temperature.

Fig. 7–10 present the temperature dependence of the maximum peak positions for LA and OA: $\nu_s(\text{CH}_2)$, $\nu_{as}(\text{CH}_2)$, $\nu_s(\text{CH}_3)$ stretching modes, and $\nu(=\text{C}-\text{H})$ vibration.

The C–H vibrations of the hydrocarbon chains are sensitive to the conformational changes, mobility and disorder-order transitions and usually exhibit distinct temperature induced changes.³⁵ One can see from Fig. 6–10 that this indeed happens for LA and OA. From the shifts of the maximum peak positions we can easily identify disorder-order transitions which occur at 222 K and 240 K for LA and at 270 K and 285 K for OA respectively.

For comparison Fig. 11 presents the changes in the maximum peak position for the C=C band crucial for unsaturated acid chain dynamics.

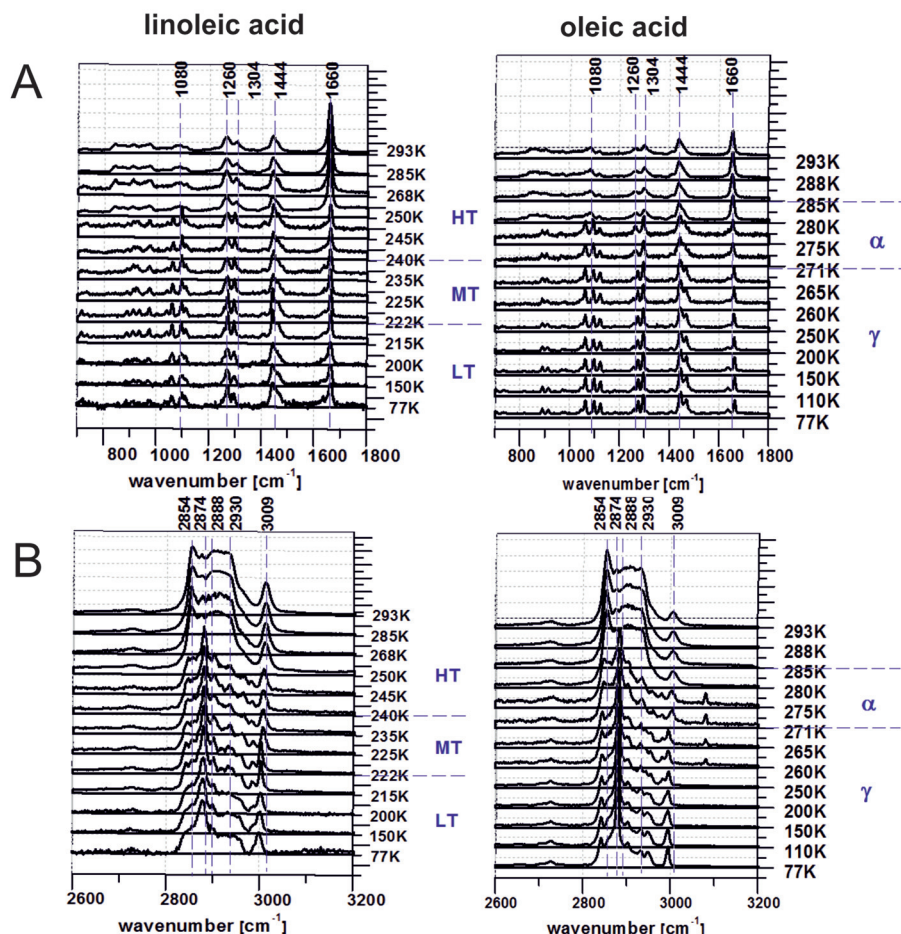


Fig. 6 Raman spectra of LA and OA as a function of the temperature in the spectral range: A: 700–1800 cm^{-1} , B: 2600–3200 cm^{-1} .

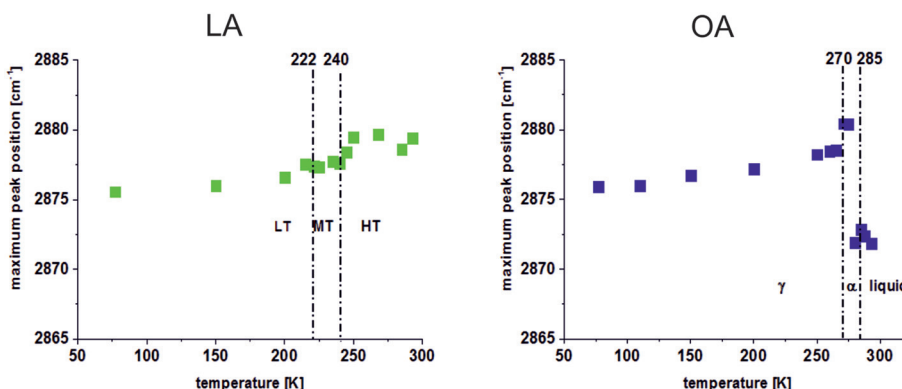


Fig. 7 The temperature dependence of the maximum peak positions for LA and OA for $\nu_s(\text{CH}_2)$ vibration.

According to the fact that the crystallographic analysis of OA and LA shows that the LT phase of LA has structural features similar to the γ phase of oleic acid,^{56–58} comparison of phase transitions between the α/γ and MT/LT can additionally elucidate how the methylene group interferes with the diene

structure of LA and affects the properties of the solid state transitions.

The cell parameters characterizing the γ phase of OA and the LT phase of LA are summarized in Table 1. One can see from Table 1 that cell parameters of OA and LA at low tempera-

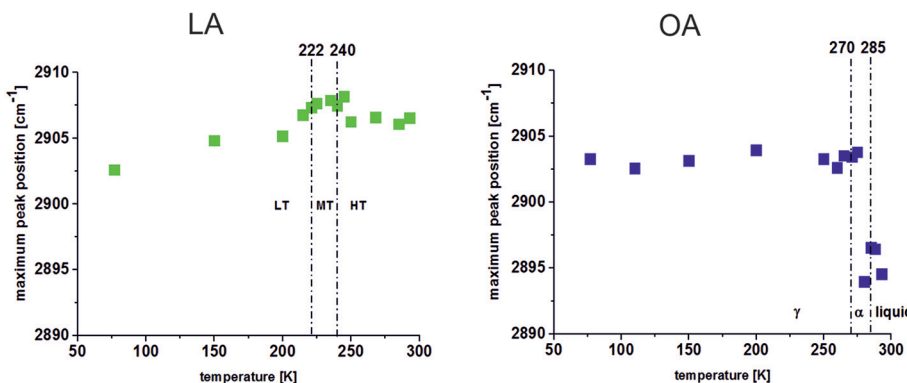


Fig. 8 The temperature dependence of the maximum peak positions for LA and OA for: $\nu_{as}(\text{CH}_2)$ vibration.

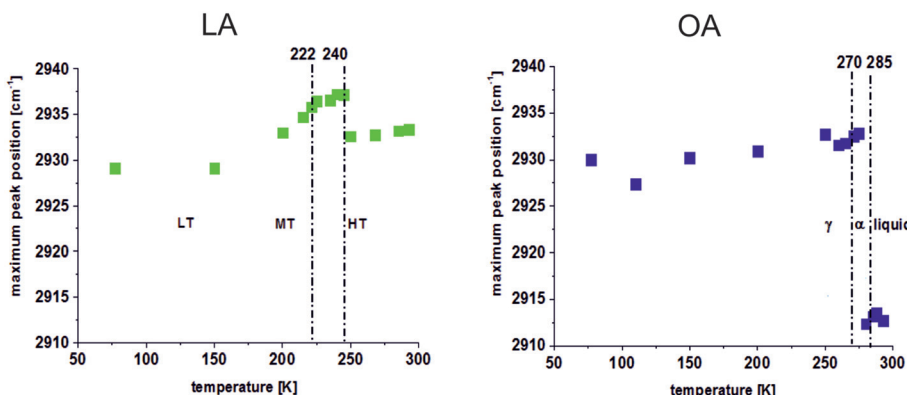


Fig. 9 The temperature dependence of the maximum peak positions for LA and OA for: $\nu_s(\text{CH}_3)$ vibration.

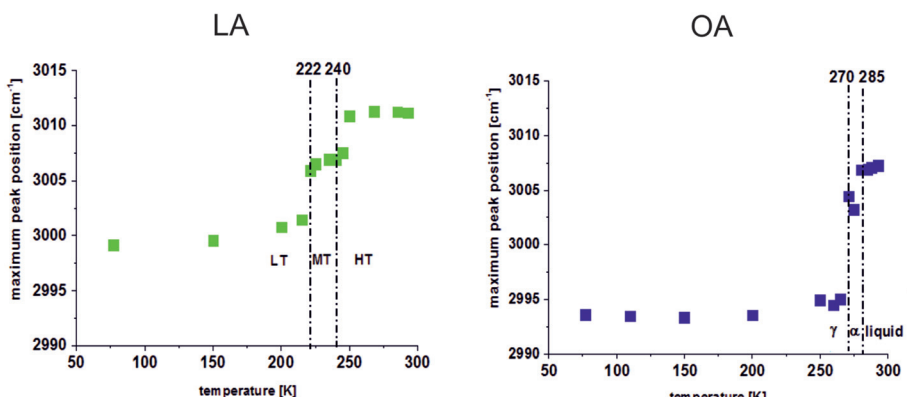


Fig. 10 The temperature dependence of the maximum peak positions for LA and OA for: $\nu_s(=\text{CH})$ vibration.

tures show many similarities and the comparison of these two phases is highly justified.

Fig. 12 presents the molecular structures of OA and LA and schematic presentation of the geometrical relationship between the monoclinic and pseudo-orthorhombic unit cell.

The structure of the γ phase of OA was determined by Abramson and Rydersteht-Nahringbauer.⁵⁷ The unit cell of OA consists of four molecules belonging to the pseudo-orthorhombic system of the space group $P2_1/a$ and the internal

rotation angles of the two C-C bonds linked to *cis* C=C are +133°, and -133°, which confirm that two all-*trans* chains on both sides of the *cis* C=C bond form the $O\parallel'$ subcell in the γ phase.⁵⁷

The structure of the LT phase of the LA was determined by Ernst *et al.*⁵⁸ The unit cell of LA consists of four molecules and similar to OA and belongs to the space group $P2_1/a$. The internal rotation angles of the four C-C bonds linked to *cis* C=C are -119°, +123°, +124°, and -121° respectively. With

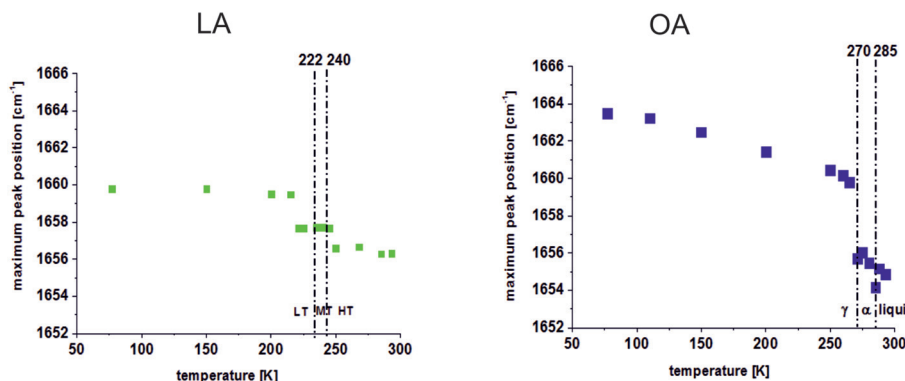


Fig. 11 Temperature dependence of the maximum peak positions of A: LA, and B: OA for the $\nu_s(C=C)$ band.

Table 1 Cell parameters of OA and LA at low temperatures⁵⁰

Acid	Space group	$a/\text{\AA}$	$b/\text{\AA}$	$c/\text{\AA}$	$\beta/^\circ$	$V/\text{\AA}^3$
OA	$P2_1/a$	9.51	4.74	40.60	~90	~1830
LA	$P2_1/a$	9.37	4.63	42.98	109.38	1761

these conformations the hydrocarbon chains are parallel to each other and the two hydrocarbon chains are packed in the $O||'$ subcell.⁵⁸

In summary LA and OA belong to the same space group. Both acids also have carboxyl side chains consisting of seven CH_2 groups. That is why the changes noticed in maximum peak positions for hydrocarbon chains are observed almost at the same frequencies (Fig. 6–11).

From Fig. 7–11 one can also notice that for C–H bonds for LA a step decreasing the maximum peak position for the MT/LT transition with the temperature decrease is observed.

Similar step changes were observed for α/γ transitions for OA.

In addition one can see from Fig. 7–11 that the spectral shifts observed for CH vibrations of LA are smaller than those for OA. It indicates that structural changes characteristic of the MT/LT transition typical of LA are smaller compared to the α/γ transition typical of OA. This can be due to the fact that the methyl side chain of LA consists of only four CH_2 groups (Fig. 12).

In other words the larger part of the OA molecule, from the *cis*-olefin to the methyl part, is involved in the phase transition. The smaller changes for the MT/LT transition for LA are also observed for $C=C$ vibrations in Fig. 11. However, for $C=C$ vibration the opposite trend with the temperature decrease was observed.

The difference in the magnitude of the spectral changes discussed above is consistent with thermodynamic data, the transition enthalpy of the MT/LT transition (2.6 kJ mol^{-1}) is about one-third of those of the α/γ transition (8.76 kJ mol^{-1}). This relationship once again suggests the smaller magnitude of structural changes in the MT/LT transition.

From Fig. 6–11 one can also notice that the phase transition temperatures typical of LA are also significantly lower (222 K,

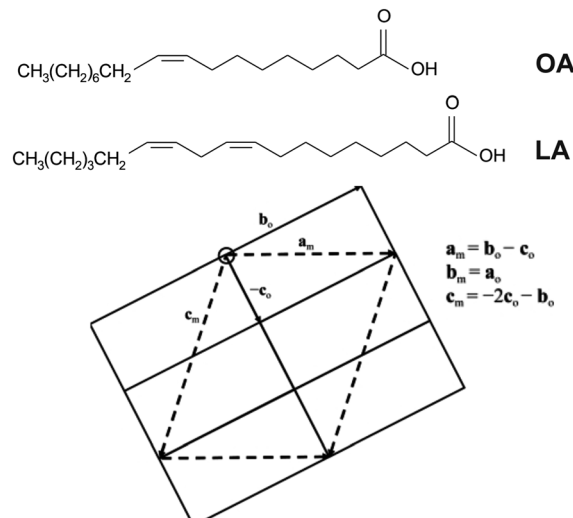


Fig. 12 Molecular structures of OA and LA and schematic presentation of the geometrical relationship between the monoclinic and pseudo-orthorhombic unit cell.

240 K) than the phase transition temperatures characteristic of OA (285 K, 270 K). When we combine results indicating smaller structural changes typical of LA transitions with the molecular structure of LA and OA and influence of the methylene group interrupting the diene structure of LA one can summarize that the C–C bonds adjacent to the *cis*- $C=C$ bond are able to adopt various rotation angles resulting in a highly flexible nature of these chains and we can regard the CH_2 group as highly mobile.

Conclusions

Some important aspects of Raman microspectroscopy analysis of noncancerous and cancerous human breast tissues and phase transitions of LA and OA in the pure state by low-temperature Raman studies have been reported. The presented studies allow the following conclusions:

1. the Raman images are sensitive indicators of distribution of fatty acids, lipids, proteins and carotenoids in cancerous and noncancerous human breast tissues,
2. noncancerous human breast tissue contains more adipose cells dominated by the unsaturated acids and their derivatives,
3. the temperature dependence of Raman spectra are sensitive indicators of phase transitions of the major components of the tissue,
4. HT/MT and MT/LT transitions for LA can be identified by Raman spectroscopy,
5. the conformational changes typical of MT/LT transitions of LA are on a smaller scale compared to parameters typical of the α/γ transition of OA.

Acknowledgements

We thank Dr Jacek Musial MD and Prof. Dr Radzislaw Kordek MD from the Medical University of Lodz for their assistance. The project was funded through a Dz. St 2014 and The National Science Centre Poland Grant UMO-2012/07/B/ST4/01588.

Notes and references

- 1 A. H. Lee and N. Hiramatsu, *Nutr. Diet. Suppl.*, 2011, **3**, 93–100.
- 2 R. K. Murray, D. K. Granner and V. W. Rodwell, *Harper's Biochemistry*, The McGraw-Hill Companies, Inc., 28th edn, 2012.
- 3 B. Brozek-Pluska, J. Musial, R. Kondek, E. Bailo, T. Dieing and H. Abramczyk, *Analyst*, 2012, **137**, 3773–3780.
- 4 L. Zhou and A. Nilsson, *J. Lipid Res.*, 2001, **42**, 1521–1542.
- 5 C. S. Koble, P. Devchand, W. Wahli, T. M. Willson, J. M. Lenhard and J. M. Lehman, *Proc. Natl. Acad. Sci. U. S. A.*, 1997, **94**, 4318–4323.
- 6 A. J. Habenicht, P. Salbach and U. Janssen-Timmen, *Eicosanoids*, 1992, **5**, S29–S31.
- 7 B. Li, C. Birdwell and J. Whelan, *J. Lipid Res.*, 1994, **35**, 1869–1877.
- 8 H. Harizi, J. B. Corcuff and N. Gualde, *Trends Mol. Med.*, 2008, **14**, 461–469.
- 9 H. Tapiero, G. Nguyen Ba, P. Couvreur and K. D. Tew, *Biomed. Pharmacother.*, 2002, **56**, 215–222.
- 10 J. A. Menedez and R. Lupu, *Nat. Rev. Cancer*, 2007, **7**, 763–777.
- 11 T. Mashima, H. Seimiya and T. Tsuruo, *Br. J. Cancer*, 2009, **100**, 1369–1372.
- 12 C. M. Metallo, P. A. Gameiro, E. L. Bell, K. R. Mattaini, J. Yang, K. Hiller, C. M. Jewell, Z. R. Johnson, D. J. Irvine, L. Guarente, J. K. Kelleher, M. G. Vander Heiden, O. Iliopoulos and G. Stephanopoulos, *Nature*, 2012, **481**, 380–384.
- 13 A. R. Mullen, W. W. Wheaton, E. S. Jin, P.-H. Chen, L. B. Sullivan, T. Cheng, Y. Yang, W. M. Linehan, N. S. Chandel and R. J. De Berardinis, *Nature*, 2012, **481**, 385–388.
- 14 G. Hatzivassiliour, F. Zhao, D. E. Bauer, C. Andreadis, A. N. Shaw, D. t. Dhanak, S. R. Hingorani, D. A. Tuveson and C. B. Thompson, *Cancer Cell*, 2005, **8**, 311–321.
- 15 R. Flavin, S. Peluso, P. L. Nguyen and M. Loda, *Future Oncol.*, 2010, **6**, 551–562.
- 16 A. Nkondjock and P. Ghadirian, *Canada. Am. J. Clin. Nutr.*, 2004, **79**, 857–864.
- 17 J. A. Menendez, L. Vellon, R. Colomer and R. Lupu, *Ann. Oncol.*, 2010, **16**, 359–371.
- 18 E. A. de Deckere, *Eur. J. Cancer Prev.*, 1999, **8**, 213–221.
- 19 Z. Gu, J. Suburu, H. Chen and Y. Q. Chen, *BioMed Res. Int.*, 2013, **2013**, 824563, DOI: 10.1155/2013/824563.
- 20 F. P. Kuhajda, *Cancer Res.*, 2006, **66**, 5977–5980.
- 21 I. M. Berquin, Y. Min, R. Wu, D. Perry, J. M. Cline, M. J. Thomas, T. Thornburg, G. Kulik, A. Smith, I. J. Edwards, R. D'Agostino Jr., H. Zhang, H. Wu, J. X. Kang and Y. Q. Chen, *J. Clin. Invest.*, 2007, **117**, 1866–1875.
- 22 C. H. MacLean, S. J. Newberry, W. A. Mojica, M. P. H. Puja Khanna, A. M. Issa, M. J. Suttorp, Y.-W. Lim, S. B. Traina, L. Hilton, R. Garland and S. C. Morton, *J. Am. Med. Assoc.*, 2006, **295**, 403–415.
- 23 P. D. Terry, T. E. Rohan and A. Wolk, *Am. J. Clin. Nutr.*, 2003, **77**, 532–543.
- 24 J. B. Ewaschuk, M. Newell and C. J. Field, *Lipids*, 2012, **47**, 1019–1030.
- 25 H. Sun, I. M. Berquin, R. T. Owens, J. T. O'Flaherty and I. J. Edwards, *Cancer Res.*, 2008, **68**, 2912–2919.
- 26 P. D. Schley, H. B. Jijon, L. E. Robinson and C. J. Field, *Breast Cancer Res. Treat.*, 2005, **92**, 187–195.
- 27 S. I. Grammatikos, P. V. Subbaiah, T. A. Victor and W. M. Miller, *Br. J. Cancer*, 1994, **70**(2), 219–227.
- 28 J. Bézard, J. P. Blond, A. Bernard and P. Clouet, *Reprod. Nutr. Dev.*, 1994, **34**(6), 539–568.
- 29 N. Salem, in *New Protective Roles for Selected Nutrients*, ed. G. A. Spiller and J. Scala, Alan R. Liss, Inc., New York, 1989, 109–228.
- 30 J. Hamilton, R. Greiner, N. Salem and H. Y. Kim, *Lipids*, 2000, **35**, 863–869.
- 31 K. Olbrich, W. Rawicz, D. Needham and E. Evans, *Biophys. J.*, 2000, **79**, 321–327.
- 32 W. Rawicz, K. Olbrich, T. McIntosh, D. Needham and E. Evans, *Biophys. J.*, 2000, **79**, 328–339.
- 33 S. E. Carlson, *Am. J. Clin. Nutr.*, 2000, **71**, 268–274.
- 34 H. Abramczyk, B. Brozek-Pluska, J. Surmacki, J. Jablonska-Gajewicz and R. Kondek, *Prog. Biophys. Mol. Biol.*, 2012, **108**, 74–81.
- 35 B. Brozek-Pluska, J. Jablonska-Gajewicz, R. Kondek and H. Abramczyk, *J. Med. Chem.*, 2011, **54**, 3386–3392.
- 36 B. Brozek-Pluska, J. Musial, R. Kondek, E. Bailo, T. Dieing and H. Abramczyk, *Analyst*, 2012, **137**, 3773–3780.

- 37 M. Iwahashi, Y. Yamaguchi, T. Kato, T. Horiuchi, I. Sakurai and M. Suzuki, *J. Phys. Chem.*, 1991, **95**, 445–451.
- 38 M. Iwahashi, N. Hachiya, Y. Hayashi, H. Matsuzawa, M. Suzuki, Y. Fujimoto and Y. Ozaki, *J. Phys. Chem.*, 1993, **97**, 3129–3133.
- 39 M. Iwahashi, Y. Kasahara, H. Matsuzawa, K. Yagi, K. Nomura, H. Terauchi, Y. Ozaki and M. Suzuki, *J. Phys. Chem.*, 2000, **104**, 6186–6194.
- 40 F. Kaneko, J. Yano and K. Sato, *Curr. Opin. Struct. Biol.*, 1998, **8**, 417–425.
- 41 F. Kaneko, K. Yamazaki, K. Kitagawa, T. Kikyo, M. Kobayashi and Y. Kitagawa, *J. Phys. Chem.*, 1997, **101**, 1803–1809.
- 42 S. Abrahamsson, B. Dahlen, H. Lofgren and J. Pascher, *Prog. Chem. Fats Other Lipids*, 1978, **16**, 125–143.
- 43 F. Kaneko, K. Tashiro and M. Kobayashi, *J. Cryst. Growth*, 1999, **198–199**, 1352–1359.
- 44 M. Kobayashi, F. Kaneko, K. Sato and M. Suzuki, *J. Phys. Chem.*, 1986, **90**, 6371–6378.
- 45 S. P. Verma and D. F. H. Wallach, *Biochim. Biophys. Acta*, 1977, **486**, 217–227.
- 46 Y. Kim, H. L. Strauss and R. G. Snyder, *J. Phys. Chem.*, 1988, **92**, 5080–5082.
- 47 S. Ueno, A. Miyazaki, J. Yano, Y. Furukawa, M. Suzuki and K. Sato, *Chem. Phys. Lipids*, 2000, **107**, 169–178.
- 48 M. Suzuki, K. Ogaki and K. Sato, *J. Am. Oil Chem. Soc.*, 1985, **62**, 1600–1604.
- 49 K. Sato and M. Suzuki, *J. Am. Oil Chem. Soc.*, 1986, **63**, 1356–1359.
- 50 F. Pi, F. Kaneko, M. Iwahashi, M. Suzuki and Y. Ozaki, *J. Phys. Chem. B*, 2011, **115**, 6289–6295.
- 51 H. Abramczyk, B. Brozek-Pluska, J. Surmacki, J. Musial and R. Kordek, *Analyst*, 2014, **139**, 5547–5559.
- 52 G. Hudelist, Ch. F. Singer, K. I. D. Pischinger, K. Kaserer, M. Manavi, E. Kubista and K. F. Czerwenka, *Proteomics*, 2006, **6**, 1989–2002.
- 53 H. Hondermarck, A. S. Vercoutter-Edouart, F. Revillion, J. Lemoine, I. el-Yazidi-Belkoura, V. Nurcombe and J. P. Peyrat, *Proteomics*, 2001, **1**, 1216–1232.
- 54 C. P. Paweletz, B. Trock, M. Pennanen, T. Tsangaris, C. Magnant, L. A. Liotta and E. F. Petricoin, *Dis. Markers*, 2001, **17**, 301–307.
- 55 R. A. Harris, A. Yang, R. C. Stein, K. Lucy, L. Brusten, A. Herath, R. Parekh, M. D. Waterfield, M. J. O'Hare, M. A. Neville, M. J. Page and M. J. Zvelebil, *Proteomics*, 2002, **2**, 212–223.
- 56 *The physical chemistry of lipids*, ed. D. M. Small, Plenum, New York, 1986.
- 57 S. Abrahamson and I. R. Nahringbauer, *Acta Crystallogr.*, 1962, **15**, 1261–1268.
- 58 J. Ernst, W. S. Sheldrick and J.-H. Fuhrhop, *Z. Naturforsch. B: Anorg. Chem. Org. Chem.*, 1979, **34**, 706–711.